NATURAL SCIENCE RESEARCH LABORATORY
TEXAS TECH
Office of the Provost
Outreach & Engagement

Occasional Papers

Museum of Texas Tech University Number 392 25 February 2025

Status, Distribution, Morphology, and Genetics of *Sigmodon fulviventer dalquesti* in the Chihuahuan Desert Ecoregion

Preston J. McDonald, Krysta Demere, Russell Martin, Jonah Evans, Robert D. Bradley, Richard D. Stevens, Mohamed Fokar, Hendra Sihaloho, and Caleb D. Phillips

Abstract

The tawny-bellied cotton rat, *Sigmodon fulviventer dalquesti*, is a Texas endemic subspecies reported only from a collection that occurred in 1991 near the town of Fort Davis in the Trans-Pecos region. The current population, distribution, and evolutionary origin of *S. f. dalquesti* is enigmatic, and its taxonomic status is uncertain. For example, the relationship among *S. f. dalquesti* and other *S. fulviventer* subspecies in Mexico, Arizona, and New Mexico is not well understood, and previous genetic comparisons only included one specimen in a phylogenetic assessment of the genus. Hence, Texas Parks and Wildlife Department's Texas Conservation Action Plan designates *S. f. dalquesti* as critically imperiled within the state and suffering from data deficiency. The current study provides a more comprehensive cranial morphometric and genetic treatment of *S. f. dalquesti*. Analysis of craniometric characters, mitochondrial cytochrome *b*, and full mitochondrial genome data presented herein support continued recognition of *S. f. dalquesti*, which is at least as distinct from the other subspecies available for comparison as the other subspecies are from each other. A potential founding source of *S. f. dalquesti* from the main *S. fulviventer* distribution is indicated by phylogenetic affinity and a two-codon insertion at the beginning of the ND2 gene shared by all *S. f. dalquesti*, and one *S. f. minimus* from northern Mexico. Distribution modeling suggests under-surveyed areas of potential range extension. However, despite multiple field surveys during this study in the area of the original detection, *S. f. dalquesti* was never captured. It is not possible to say if this reflects extinction or a population size occurring below the limit of detection during the survey period.

Key words: *Sigmodon fulviventer dalquesti*, Species of Greatest Conservation Need, Trans-Pecos ecoregion

Supplementary material related to this manuscript is available online at: https://github.com/genotyper/S.f.dalquesti.

INTRODUCTION

In March of 1991, a population of *Sigmodon fulviventer* (J. A. Allen, 1889) was discovered by Dr. Frederick B. Stangl, Jr., in Jeff Davis County, Texas (Stangl 1992a). Twenty individuals, including four pregnant females, were captured (Stangl 1992a) at a single locality. At the time, Stangl reported that this represented an extension of more than 100 km eastward from the known range limit of *S. fulviventer* in New Mexico (Stangl 1992a). Since Stangl's initial discovery, no further captures or observations of this species have been made in the state of Texas. The initial captures took place in late March 1991, with additional trapping in May 1991 failing to produce additional captures (Stangl 1992a, b). Subsequent trapping efforts reported by Stangl in the same year as the first detection failed to produce more captures, and Stangl speculated that the species may be rare in the area, and subject to high seasonal variability in population (Stangl 1992b).

Stangl (1992b) formally described the specimens of Texas *S. fulviventer* as an endemic subspecies, *S. f. dalquesti*. This taxonomic revision was based on craniometric and pelage comparisons between the series of specimens taken in Jeff Davis County (N=7), and a series of *S. f. minimus* (N=12) taken in New Mexico near the main *S. fulviventer* distribution closest to the Texas captures. Although supportive of subspecific status, the craniometric comparisons involved relatively small numbers of individuals, reported only means and ranges for five selected characters, and no assessments of statistical significance of group differences were made (Stangl 1992b). Other recognized subspecies include *S. f. minimus*, *S. f. fulviventer*, *S. f. melanotis*, and *S. f. goldmani* (Baker and Shump 1978), and the general validity of subspecies distinctions were supported in a common garden experiment finding that statistically significant differences in a number of craniometric characters were maintained between *S. f. minimus*, *S. f. fulviventer*, and *S. f. melanotis* when reared in the same environment (Baker 1969). Further, Baker (1969) noted the existence of a pelage coloration cline that he considered concordant with the morphometric evidence and in agreement with the recognized subspecies boundaries between *S. f. minimus* and *S. f. fulviventer* in Durango, Mexico, and *S. f. fulviventer* and *S. f. melanotis* in Guanajuato-Jalisco, Mexico. Findley and Jones (1963) concluded based on unique pelage characteristics that *S. f. goldmani*, originally described by Bailey (1913) based on three specimens, is indeed a recognizable subspecies but suggested that the population was extinct given its absence from, and presence of *S. hispidus*, at the type locality in central New Mexico. Overall, the cumulative previous efforts characterizing distinction among subspecies provides a useful comparator to further evaluate *S. f. dalquesti*.

In the intervening years since Stangl's discovery, no additional captures have been reported, nor do digitized collections including the Global Biodiversity Information Facility, VertNet, and Arctos databases include additional *S. fulviventer* from Texas. As a result, the extent of *S. f. dalquesti* occurrence in the state is poorly known (Stangl 1992b; Schmidly and Bradley 2016). For this reason, the Texas Conservation Action Plan (2012) ranks the tawny-bellied cotton rat as Critically Imperiled within the state, although *S. fulviventer* as a whole is not currently considered to be under threat and is classified as Least Concern (Álvarez-Castañeda et al. 2016). Whereas Texas listing of *S. f. dalquesti* was agnostic to its subspecific status, but rather based upon its assumed limited distribution and population size within the state, subspecies as infraspecific taxonomic designations are relevant categories in conservation law including the Endangered Species Act of 1973. Thus, more detailed assessment of the validity *S. f. dalquesti* would help inform conservation as necessary.

The use of the subspecies rank in taxonomy has been controversial due to the regularly non-discrete nature of character variation within species (reviewed in Beauchamp-Martin et al. 2019). Ernst Mayr (1999) presented a definition of subspecies as geographically isolated, taxonomically differing populations of an interbreeding species, which could be distinguished based on morphological traits that were genetic, rather than environmental, in nature. Geographic variation in a chosen character or set of characters is often gradual, therefore the degree of variation between two populations that is sufficient to justify recognition of subspecies must be arbitrary (Amadon 1949). A widely used criterion is the 75% rule mentioned by Mayr (1982) and treated in detail by later workers (Pimentel 1959;

Amadon 1949; Patten 2015). For the purpose of this study, the rule has been interpreted in the strict sense as described by Amadon (1949), meaning that the degree of differentiation between populations in a given morphological character is sufficient to support subspecies classification if 97% of the character distribution of one population lies outside 97% of the other population. Debate about the validity and usefulness of subspecies classification continues, but in practice the rank has practical application (Patten 2015).

Given the state-level conservation listing of *S. f. dalquesti* in conjunction with the limited information available about *S. f. dalquesti* distinctness, a primary aim of this study was to evaluate the validity of its subspecific status through joint consideration of craniometric and genetic characters. Because *S. f. dalquesti* is only known from a single event more than 30 years ago, an additional goal of this work was to provide an improved understanding of continued existence and potential range of the tawny-bellied cotton rat in Texas using a combination of field surveys and distribution modeling.

Materials and Methods

Morphometrics

Measurement.—Cranial character measurements were taken using Mitutoyo Absolute Digimatic Calipers (0–150 mm). Following published descriptions (Carleton 1982) of craniometric methods in mammals, cranial characters measured were greatest length of the skull (GLS – measured from the anterior of the nasal to the most posterior point of the occipital), zygomatic breadth (ZB – the greatest breadth across the zygomatic arches), breadth of braincase (BB – measured as the breadth across the cranium at the constriction immediately posterior to the zygomatic arches), mastoid breadth (MB – greatest breadth across the skull at the mastoid processes), least interorbital width (LIW – narrowest length across the frontal bones measured at the interorbital constriction), rostral breadth (RB – greatest breadth across the premaxilla immediately posterior of the incisors), rostral length (RL – measured from the tip of the nasals to a line across the posterior margins of the third molars), post-palatal length (PPL – measured from the anterior most on the posterior edge of the right palatal bone to the anterior most point on the foramen magnum), length of the incisive foramina (LIF – internal length of the right incisive foramen), length of the bony palate (LBP – measured from the anterior alveolus between the incisors to the anterior margin of the posterior edge of the right palatal bone), greatest breadth across the molars (GBM – breadth across the molars at the lateral alveolae of the second molars), length of the molar tooth row (LMT – length from the anterior alveolus of the first molar to the posterior alveolus of the third molar on the right side tooth row), post-dental palatal breadth (PPB – least breadth across the post-dental constriction of the palatal bones), length of the auditory bullae (LAB – greatest length of the long axis of the right auditory bulla), length of the mesopterygoid fossae (LMF – greatest length of the lateral process of the right pterygoid), width of the mesopterygoid fossae (WMF – greatest length across the posterior most points of the lateral processes of the pterygoids), nasal length (NL – greatest length from the posterior tip to the anterior most point of the suture of the nasals at the midline), and depth of the braincase (DB – greatest height of the skull with the skull resting on a flat surface) (Figure 1; Carleton et al. 1999; Martin et al. 2011). Measurements were taken from voucher specimen collections at the following institutions: Midwestern State University, Wichita Falls, Texas; Museum of Vertebrate Zoology, University of California, Berkeley; Museum of Southwestern Biology, University of New Mexico, Albuquerque; National Museum of Natural History, Smithsonian, Washington, DC; and the Museum of Texas Tech University, Lubbock (Fig. 1, Supplementary Data 1, Supplementary Data 2). Measurement data was recorded in tabular format in Microsoft Excel and exported for statistical analysis in R 3.5.1.

The age at death of each specimen on a 6-point scale was estimated by visually examining the condition of the teeth. Similar methods have been successful in determining the approximate ages of mammals (Findley and Jones 1963; Schmidly 1973; Carleton et al. 1999).

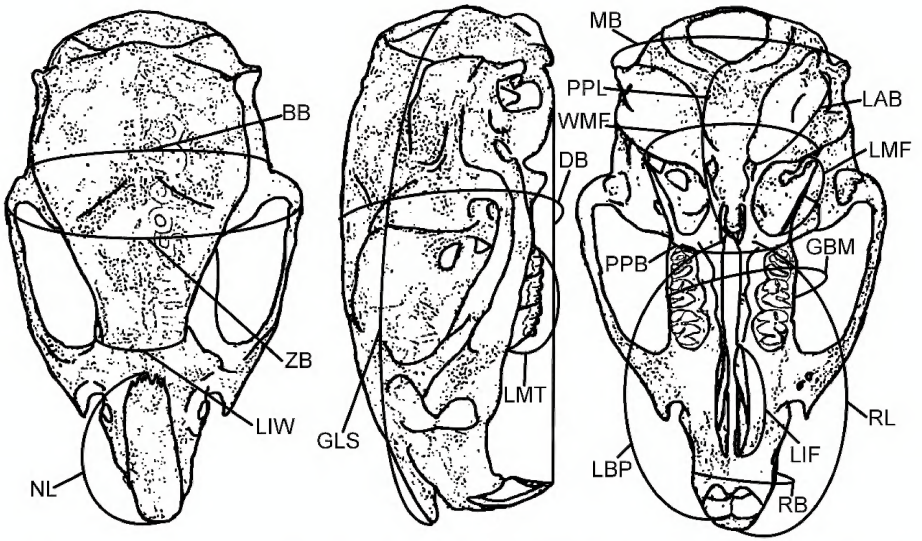

Figure 1. Craniometric characters measured: greatest length of the skull (GLS), zygomatic breadth (ZB), breadth of braincase (BB), mastoid breadth (MB), least interorbital width (LIW), rostral breadth (RB), rostral length (RL), post-palatal length (PPL), length of the incisive foramina (LIF), length of the bony palate (LBP), greatest breadth across the molars (GBM), length of the molar toothrow (LMT), post-dental palatal breadth (PPB), length of the auditory bullae (LAB), length of the mesopterygoid fossae (LMF), width of the mesopterygoid fossae (WMF), nasal length (NL), and depth of the braincase (DB).

The tooth condition scale is summarized in Supplementary Data 3, with examples in Supplementary Data 4.

Analysis.—Qualitative validation of the age categories was accomplished using a calibration curve (see Supplementary Figure 5). The calibration curve is a digitized reproduction of a portion of Figure 3 from R. H. Baker's review, which plots condylo-premaxillary length (CPL) against the age of captive animals in days, as well as means and ranges reported for lab-raised *S. fulviventer* (Baker 1969; Jimenez 1972). Observed values of CPL were estimated as the sum of PPL and LBP, and predicted ages were inferred from the curve. This plot provides a visual confirmation that the tooth wear-based age categories correspond to the approximate age of the animal, and that the choice of category for each animal comports with previous observations of the correspondence of tooth wear and age in this species. Findley and Jones (1963) found that *S. fulviventer* in New Mexico are full sized when at least one molar reentrant angle had been isolated as a loop of enamel surrounded by exposed dentine. This condition corresponds to age category 5 in this study. The correspondence between age category and chronological age seems closer for younger animals, and age category underestimates age for older animals, likely owing to increasing inter-individual variability in accumulated tooth wear over the life of individuals, and to the fact that the curve was created with data from animals reared in captivity (Baker 1969). Baker (1969) proposed that cottons rats less than 75 days old should be considered juveniles, however, he also reported that the same lab-reared *S. fulviventer* used to generate his growth curves had produced offspring as young as 77 days, likely having mated around 42 days old. He also relayed the results of prior studies on cotton rat life history that suggest that hispid cotton rats begin breeding by two months of age (Odum 1955; Baker 1969). For this reason, it seems reasonable to conclude that age category 4–6 represent adults.

Outlier screening was conducted for each cranial character by identifying observations laying more than three times the interquartile range above or below the 3rd and 1st quartiles, respectively, within each age category, sex, and subspecies. Of these, those that were obviously the result of data entry error, i.e., with values exactly equal to nearby cells in the table, were deleted and treated as missing data (MSU10462, LAB; TK72440, RL). The remaining unexplained outliers were left untreated, as no statistical justification could be found for their exclusion. Data were then log transformed to facilitate statistical analyses.

Missing cranial character observations were handled using multivariate imputation by chained equations as implemented in the MICE package (van Buuren and Groothuis-Oudshoorn 2011). This method imputes missing values by iteratively regressing a variable with missing values on all other supplied variables as predictors. All cranial measurements were imputed using all other cranial characters, age category, sex, latitude, longitude and collection date as predictors. Age category, sex, latitude, longitude, and collection date were not imputed. The imputed dataset was used in downstream analyses. The number of individuals in each age, sex, and subspecies used in the downstream analyses is summarized in Table 1.

The null hypotheses that no differences in cranial characters exist across subspecies, sexes, and age classes, were tested using permutational multivariate analysis of variance as implemented in the vegan package (Anderson 2001; Anderson 2006; Anderson 2017; Oksanen et al. 2018). The underlying assumption of homogeneity of multivariate dispersion was tested using the PERMDISP2 method, also implemented in vegan (Anderson et al. 2006; Anderson 2017; Oksanen et al. 2018). The Benjamini-Hochberg method was

Table 1. The number of individuals in each age, sex, and subspecies for morphometric analysis.

		Age Category						
Subspecies	Sex	1	2	3	4	5	6	Totals
dalquesti	F	2	1	3	2	2	1	11
	M	5	0	0	1	0	1	7
								18
fulviventer	F	0	1	2	0	1	0	4
	M	0	1	1	0	1	0	3
								7
melanotis	F	0	2	3	1	0	0	6
	M	1	2	3	2	0	0	8
								14
minimus	F	9	9	8	7	7	1	41
	M	4	13	14	3	8	4	46
								87
							Total	126

used to control the false discovery rate for multiple comparisons (Benjamini and Hochberg 1995).

To identify candidate variables to diagnose *S. f. dalquesti* from *S. f. minimus*, univariate PERMANOVA tests were conducted on each cranial character, and terms with significant subspecies effects after Benjamini-Hochberg correction were selected. These terms were used to create a linear discriminant function maximally separating adult individuals (age categories 4–6) using the MASS package (Venables and Ripley 2002).

Molecular Phylogenetics

DNA extraction.—Genomic DNA was extracted from voucher specimens and frozen tissue samples provided by the Museum of Texas Tech University, the Museum of Vertebrate Zoology, Midwestern State University, and the Museum of Southwestern Biology (Supplementary Data 6). If tissue was not available, material from voucher specimens consisted of either a single toe clipping taken at the joint of the distal phalange on one hind foot or of a 25 mm^2 skin clipping taken from the ventral incision of the study skin. The extraction protocol for toe and skin samples was adapted from previously published methods for DNA extraction from voucher specimen material (Campos and Gilbert 2012; McDonough et al. 2018). DNA extraction from tissue samples followed the standard extraction protocol supplied with the Qiagen DNEasy Blood and Tissue extraction kit.

PCR amplification.—Cytochrome *b* amplification was conducted using the manufacturer provided ThermoFisher Scientific Phire Hot Start II DNA Polymerase (cat. F122S) amplification protocol on an Eppendorf Mastercycler Pro (prod. number 950030010). For frozen tissue-derived extractions, previously developed primers were used to amplify the full cytochrome *b* gene (Bickham et al. 1995). For toe- and skin-derived extractions, an additional collection of internal primers was designed using Primer3 (Supplementary Data 7) (Koressaar and Remm 2007; Untergasser et al. 2012). These primers targeted 200–300 base pair regions overlapping by approximately 50 base pairs.

Cytochrome b *sequencing.*—BigDye Sanger sequencing of cytochrome *b* was conducted commercially using the services of Sequetech (Mountain View, California; Applied Biosystems 3730xl DNA Analyzer). The sequence data in AB1 format were edited by visual inspection of the base calls and chromatograms using the UGENE software package (Okonechnikov et al. 2012). Reads were aligned by reference guided alignment using the *Sigmodon hispidus* reference mitochondrial genome (NC_035572.1) in AliView (Larsson 2014; Sullivan et al. 2017). Published sequences for *Sigmodon leucotis* (AF293401, EU652909) also were aligned for subsequent use as the outgroup (Peppers et al. 2002; Henson and Bradley 2009;).

Mitochondrial genome sequencing.—For a subset of specimens (16 of 26; Supplementary Data 6), approximately 250 ng DNA was taken for shotgun DNA library preparation targeting 350 bp median peak insert sizes. Celero EZ DNA-Seq kit (Tecan Genomics, Inc., California, USA) was used for libraries following manufacturer protocol. Briefly, libraries were prepared by 30-minute enzymatic fragmentation, then unique barcodes for each sample were ligated followed by six cycles of PCR amplification. Library purification was performed after amplification using Ampure XP (Beckman Coulter, Inc., Indiana, USA) magnetic beads with 0.75X bead ratio and following the Celero EZ DNA-seq library preparation procedure. Each library was analyzed on a Qubit fluorometer (Life Technologies, California, USA) for concentration and on a Tapestation (Agilent Technologies, Inc., Califiornia, USA) for fragment size distribution. Molarity of each library was determined based on Qubit and Tapestation results, and the volumes for equal molarity among pooled libraries were calculated. Pooled libraries also were measured with Qubit and Tapestation before 2 x 100 bp sequencing on Novaseq 6000 (Illumina, Inc.) at the Center for Biotechnology and Genomics, Texas Tech University.

Analysis.—Pairwise cytochrome *b* Kimura 2-parameter distances were calculated using MEGA (Kumar et al. 2016). A PCoA also was used to visualize the distances. Mitochondrial genomes were assembled using GetOrganelle version v1.7.5 (Jin et al. 2020). Assembly was guided by a published complete mitochondrial genome of *Sigmodon hispidus* (GenBank: KY707311.1). Because of sequence overlap at the ends of the KY707311.1 fasta, the overlapped bases were deleted from one end to produce a non-overlapping seed file using circle_check.py from MitoZ v2.3 (Meng et

al. 2019). Then, the genes and seed files were prepared using the non-overlapping fasta and python script get_annotated_regions_from_gb.py of GetOrganelle software. The settings R 10, -k 21, 45, 65, 85, and 105 for GetOrganelle were used for reference-guided assembly. Each mitochondrial assembly result was assessed for completeness by visualization using Bandage v0.8.1 (Wick et al. 2015). Some samples were not assembled completely using the describe method above. Those samples produced a non-circular genome when visualized using Bandage software. To obtain complete mitogenome for those difficult samples, de-novo assembly was done by SPAdes v3.13.0 (Prjibelski et al. 2020) using same kmer setting as above, then the fastg file produced by SPAdes was employed by get_organelle_from_assembly.py from GetOrganelle.

Raw reads were mapped back to assembled genomes for each individual with bwa (Li and Durbin 2009), and fold-coverage was extracted with samtools 1.9 (Danecek et al. 2021). Annotation of assembled files was carried out using Mitos v2 online tool (Donath et al. 2019). Mitochondrial chromosomes were aligned using MAFFT v7.490 (Katoh and Standley 2013). A phylogenetic tree was estimated using maximum likelihood on RAxML v.8.2.12 (Stamatakis 2014) with settings -n bootstrap -m GTRGAMMA -p 123 -f a -N 200 -x 456, and *S. leucotis* was treated as an outgroup.

Field effort.—To investigate if the population discovered by Stangl (1992a) is extant, small mammal surveys in the Trans-Pecos region of Texas were conducted. The original locality was included, as were other sites in Jeff Davis and Presidio Counties that contain suitable habitat. Trapping methodology consisted of Sherman trap surveys positioned opportunistically to cover habitat areas that appeared suitable for cotton rats. A summary of captures and field effort is provided in Supplementary Data 8 and Supplementary Data 9, respectively.

Fieldwork and animal sacrifices were conducted in accordance with established guidelines and Texas Tech University policies under IACUC protocol #17023-02 (Leary et al. 2013; Sikes 2016). Animals were prepared as voucher specimens for deposition in the Natural Science Research Laboratory of the Museum of Texas Tech University. Permits for scientific collection were obtained from the Texas Parks and Wildlife Department (SP-0393-593). Permission to collect on private lands, the Mimms Unit of the Dixon Water Foundation, and the Chihuahuan Desert Research Institute also was obtained.

Species Distribution Modeling

Occurrence records.—The entire collection of GBIF records for preserved specimens or material samples representing family Cricetidae were downloaded and filtered to dates in the range 1980–2019 within Mexico, Arizona, New Mexico, and Texas (GBIF.org; Supplmentary Data 10). Records that lacked locality and geographic coordinates, or lacked species identifications, were excluded. The remaining records were cross-checked by mapping using QGIS v3.4.13. The records were split into three files, one of which contained 96,324 records of Cricetidae excluding *Ondatra* and *Neofiber*, one containing 192 records of *Sigmodon fulviventer*, and one containing 188 records of *S. fulviventer* excluding *S. f. dalquesti*. All following references to occurrence records refer to these cleaned files.

Environmental data.—Two sets of geographic data were used to build a maximum entropy species distribution model using MaxEnt (Phillips et al. 2006, 2017). All geographic data sources used were at the 30 arc second scale, approximating 1 km^2 using the WGS84 datum. All data layers were clipped to the chosen study area of Mexico, Arizona, New Mexico, and Texas counties lying within or partially within the High Plains, Edwards Plateau, or South Texas Plains. The first set consisted of variables used to approximate a model of sampling bias for the target group Cricetidae. Following established methods, a bias model was generated by building a distribution model for the Cricetidae records using distance to roads, population density, distance to nearest populated area with $\geq$ 10,000 people, topographic roughness, and country (S. J. Phillips et al. 2009; Merow et al. 2013; Hijmans 2018; Center for International Earth Science Information Network 2013, 2018a, b; Amatulli et al. 2018). The second set of geographic data was used to build the distribution model for *S. fulviventer*. Predictor variables comprised elevation, slope, EPA Level III terrestrial ecoregion, North American Land Change Monitoring System land cover data, and all 19 Bioclim variables (Commission for Environmental Cooperation 2009; Canada Centre

for Remote Sensing et al. 2013; Fick and Hijmans 2017; Amatulli et al. 2018).

Analysis.—The sampling effort bias model layer was produced using the previously mentioned environmental data and occurrence records for Cricetidae. The resulting model represents sampling effort bias as a function of human population density, distance to the nearest road, distance to the nearest population center, topographic roughness, and country (Supplementary Data 11). Default settings were used excepting that the regularization parameter was set to 3, and 10-fold cross validation was used to test model performance.

The species distribution model was produced using the previously described environmental data layers, and separate models were created using the *S. fulviventer* records with and without *S. f. dalquesti* occurrences. The default settings were used with the exception that the regularization parameter was set to 5, and 4-fold cross validation was used to test model performance.

RESULTS

Morphometrics

No significant differences in dispersion were found between sexes ($F=0.0743$, $p>0.783$). No significant differences in dispersion across age categories were found, except for pairwise tests 6 vs 1 and 6 vs 3 were found to have significant differences in dispersion (Table 2). Examination of a principal coordinates analysis plot revealed that the likely source of the difference in dispersion is the reduced sample size of category 6 relative to the other categories (Fig. 2A). A significant difference in dispersion across subspecies was found, and examination of the pairwise tests and the PCoA plot show this difference is likely to be due to the low number of individuals of *S. f. fulviventer* and *S. f. melanotis* (Table 3, Fig. 2B).

The PERMANOVA including all subspecies found significant effects of age category and subspecies ($F=55.21$, $p<0.01$ and $F=7.52$, $p<0.01$ respectively). In agreement with previous literature, no significant effect of sex was found (Baker and Shump 1978; Carleton et al. 1999). No interaction terms were significant. Pairwise PERMANOVA for each pair of subspecies found a significant effect of subspecies, with the exceptions of *S. f. dalquesti* vs. *S. f. melanotis* and *S. f. minimus* vs. *S. f. fulviventer* (Table 4). P ost-hoc PERMANOVA tests of each cranial variable (with Benjamini-Hochberg corrections) identified a list of candidates to build a proposed composite variable to use for subspecies diagnosis that included LIF, NL, LAB, PPB, DB, GLS, LMF, RL, and LBP. A linear discriminant function analysis was conducted using these variables. Scores of individuals along the resulting axis were plotted. As a significant effect of subspecies was found in the PERMANOVA, but no effect of an age-by-subspecies interaction, it was concluded that ontogenetic differences across subspecies may be ignored, and therefore age categories 4–6 were combined and sex was ignored for the linear discriminant analysis (Fig. 3).

Molecular Phylogenetics

Among 26 *S. fulviventer* included in *Cyt*b sequencing, 44 variable sites were identified, of which 25 were parsimony informative. Consensus mitochondrial genomes among 16 *S. fulviventer* were based on a median coverage of 355 reads per base position (minimum = 143, 1st quartile = 275, 3rd quartile = 3881, max = 6,013). The mitochondrial genome alignment was 15,915 base pairs in length consisting of 421 variable sites, of which 202 were parsimony informative. Three gap regions were identified, one within the origin of replication, a second within the 16S locus, and a final six base pair insertion/deletion at the beginning of the ND2 gene. All *S. f. dalquesti* and one *S. f. minimus* from northern Mexico (MVZ128460) shared the 6 base pair insertion which results in additional N-terminus methionine and leucine residues in these lineages. The consensus mitochondrial genome tree produced by RAxML is presented in Figure 4 with labels as bootstrap support for each node. *Sigmodon f. dalquesti* specimens plus MVZ128460 formed a clade with 98 percent bootstrap support, positioned within a poorly supported *S. f. minimus* clade. The remaining *S. f. minimus* and all *S. f. fulviventer* were positioned in the remainder of the tree. Pairwise genetic distances at *Cyt*b were nominally greatest in comparison between *S. f. dalquesti* and *S. f.*

Table 2. Result of test of dispersion across age categories.

	Df	Sum Sq.	Mean Sq.	F	N. Perm.	p
Age Category	5.00	0.14	0.03	1.44	999	0.23
Residuals	124.00	2.37	0.02			

Pairwise comparisons:
(Observed p-value below diagonal, permuted p-value above diagonal)

	1	2	3	4	5	6
1		0.70	0.94	0.68	0.13	0.04
2	0.67		0.68	0.89	0.24	0.06
3	0.95	0.67		0.63	0.08	0.02
4	0.65	0.90	0.64		0.42	0.16
5	0.11	0.22	0.08	0.39		0.24
6	0.04	0.06	0.02	0.15	0.23	

Table 3. Result of test of dispersion across subspecies.

	Df	Sum Sq.	Mean Sq.	F	N. Perm.	p
Subspecies	3	0.73	0.24	3.64	999	0.02
Residuals		8.41	0.07			

Pairwise comparisons:
(Observed p-value below diagonal, permuted p-value above diagonal)

	dalquesti	*fulviventer*	*melanotis*	*minimus*
dalquesti		0.00	0.04	0.47
fulviventer	0.00		0.28	0.02
melanotis	0.04	0.26		0.08
minimus	0.46	0.01	0.07	

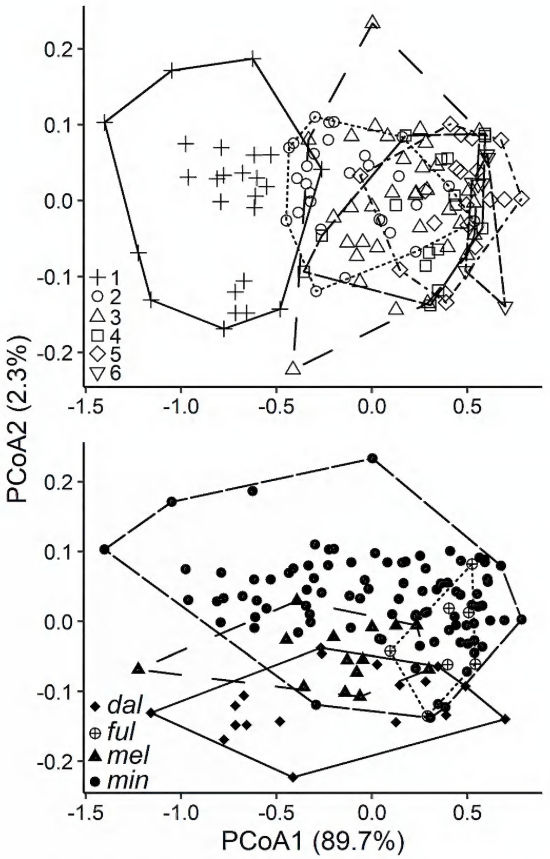

Figure 2. Principal coordinates analysis of cranial characters, subset by age category (A), and by subspecies designation associated with each museum specimen (B). Shapes refer to age categories 1–6 for A, and subspecies in B. The percentage of correlated craniometric variation explained by each axis is provided.

Table 4. Pairwise PERMANOVA results between subspecies. Reported p-value corrected for multiple comparisons using Benjamini-Hochberg method.

Ssp. Pairs	Terms	Df	Sum Sq.	R2	F	p corr.
dalquesti X *fulviventer*	Age Category	5	5.51	0.74	14.25	0
	Subspecies	1	0.61	0.08	7.85	0.02
	Age Cat. by Ssp.	2	0.07	0.01	0.48	0.73
	Residual	16	1.24	0.17		
	Total	24	7.43	1		
dalquesti X *melanotis*	Age Category	5	5.32	0.7	12.58	0
	Subspecies	1	0.11	0.01	1.28	0.35
	Age Cat. by Ssp.	3	0.28	0.04	1.09	0.45
	Residual	22	1.86	0.25		
	Total	31	7.57	1		
dalquesti X *minimus*	Age Category	5	21.93	0.72	57.68	0
	Subspecies	1	0.62	0.02	8.17	0
	Age Cat. by Ssp.	5	0.47	0.02	1.24	0.35
	Residual	97	7.38	0.24		
	Total	108	30.4	1		
fulviventer X *melanotis*	Age Category	4	2.23	0.57	8.01	0
	Subspecies	1	0.71	0.18	10.23	0
	Age Cat. by Ssp.	1	0.01	0	0.2	0.81
	Residual	14	0.97	0.25		
	Total	20	3.92	1		
fulviventer X *minimus*	Age Category	5	18.12	0.72	49.72	0
	Subspecies	1	0.29	0.01	3.96	0.07
	Age Cat. by Ssp.	2	0.12	0	0.84	0.48
	Residual	89	6.49	0.26		
	Total	97	25.02	1		
melanotis X *minimus*	Age Category	5	18.31	0.69	48.91	0
	Subspecies	1	0.89	0.03	11.83	0
	Age Cat. by Ssp.	3	0.36	0.01	1.61	0.24
	Residual	95	7.11	0.27		
	Total	104	26.67	1		

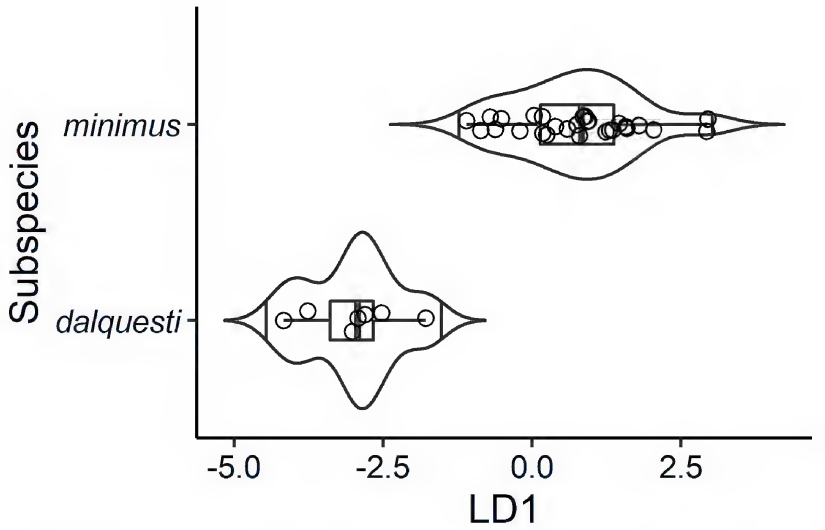

Figure 3. Results of linear discriminant analysis using selected cranial characters. The proposed discriminant function is LD1 ≈ 11logLIF + 12logNL - 7logLAB - 27logPPB + 8logDB - 23logGLS - 10logLMF + 16logRL + 14logLBP. Vertical lines in kernel density estimate represent 3% and 97% quantiles. Distributions are illustrated as box and whisker plots defined by 25th and 75th quartiles, with vertical lines within boxes indicating medians, and whiskers calculated as 1.5 times the interquartile range. Violin plots are overlaid to illustrate the density of sample points at each location on the x-axis.

fulviventer, and smallest within *S. f. dalquesti* (Table 5). The PCoA of the genetic distances is provided in Supplementary Data 12.

Species Distribution Modeling

The mean area under the receiver operating curve (AUC) for the species distribution model was 0.895, with a standard deviation of 0.006. The resulting species distribution is presented in Supplementary Figure 5. The full distribution model is available for download at https://github.com/genotyper/S.f.dalquesti.

Table 5. Mean Kimura 2-parameter cytochrome-*b* distances by subspecies.

	dalquesti (n=6)	*fulviventer* (n=6)	*minimus* (n=14)
dalquesti	0.13	1.59	0.62
fulviventer		0.36	1.41
minimus			0.73

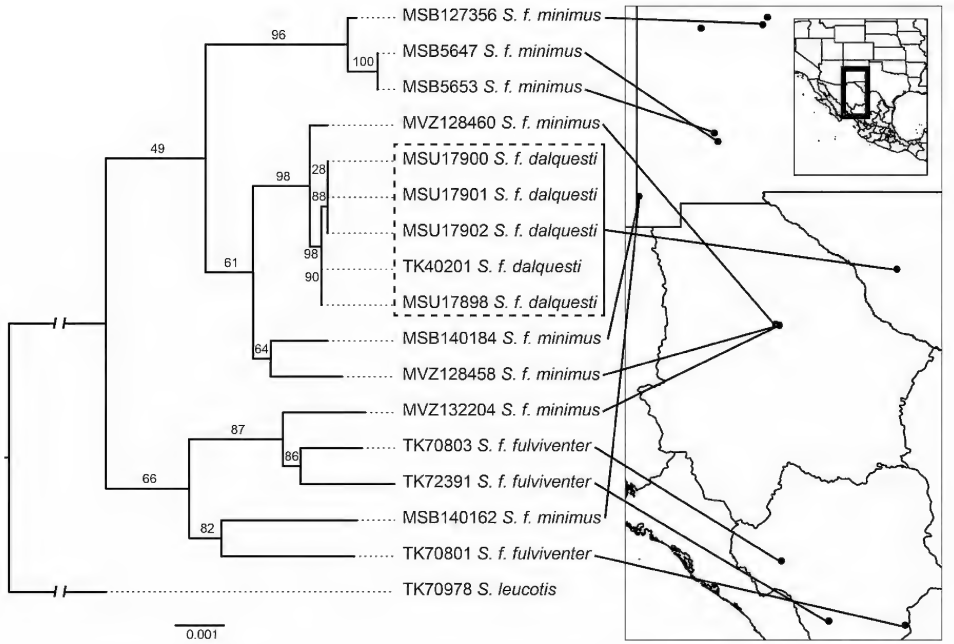

Figure 4. Maximum likelihood gene tree of mitochondrial genomes for *S. fulviventer* ssp. Numbers represent bootstrap support. Map locations represent localities of specimens.

DISCUSSION

This study was conducted following a commonly used operational definition of subspecies as a population that is geographically circumscribed, morphologically diagnosable by a concordant set of characters, genetically distinct from conspecific populations, but not meeting the requirements of species delimitation under a suitable species concept (Mayr 1982, 1999; Patten and Unitt 2002; Phillips et al. 2009). The results of the analysis show that the chosen cranial characters are sufficient to statistically distinguish *S. fulviventer* ssp. when analyzed in a multivariate framework. Each subspecies included in the analysis was found to represent a statistically significant population in morphological space as compared to the others, with the exceptions of *S. f. dalquesti* vs. *S. f. melanotis* and *S. f. minimus* vs. *S. f. fulviventer*. This result suggests that for these characters, *S. f. dalquesti* cannot be distinguished statistically from *S. f. melanotis*. The practical significance of this result is not immediately clear. The original description of *S. f. dalquesti* noted an overall darker dorsal pelage relative to *S. f. minimus*, a comparison that also holds for *S. f. melanotis* relative to *S. f. minimus* (Baker 1969; Stangl 1992b). Together, this result and the prior reported coloration suggest the possibility of overall morphological similarity between *S. f. dalquesti* and *S. f. melanotis*, the cause of which cannot be resolved with this dataset. Some possible explanations include coincidence due to population level drift effects, convergence due to similar local conditions in each respective subspecies' portion of the species' range, or the possibility that *S. f. dalquesti* represents a recent (possibly human-assisted) dispersal from *S. f. melanotis*'s portion of the range. The great distance between the populations of *S. f. dalquesti* and *S. f. melanotis* makes this seem unlikely.

These possibilities will from here be set aside to focus on the comparison between *S. f. minimus* and *S. f. dalquesti*, which is of greater practical significance in answering the question of diagnosable difference due to the large geographic distance between *S. f. dalquesti* and *S. f. melanotis*. The analyses described above showed that this pair is statistically distinguishable using all the measured variables together. As can be seen in the linear discriminant analysis (Fig. 3), the difference between *S. f. dalquesti* and *S. f. minimus* is sufficient to distinguish ≥75% of each subspecies from the other using this composite variable, satisfying the established 75% percent rule for diagnosis (Amadon 1949; Rand and Traylor 1950; Pimentel 1959; Patten and Unitt 2002). Additionally, two characters included in the original description of *S. f. dalquesti* were not included, basioccipital length and bullar width (Stangl 1992b). Furthermore, the possibility that the variation is clinal in nature is not addressed in this study because doing so would require samples uniformly distributed across the geographic extent of the species range, which are unavailable. Nevertheless, it seems reasonable to conclude that the totality of the morphological evidence suggests the diagnosability of *S. f. dalquesti*, at least as compared to *S. f. minimus*. The strength of this conclusion could be improved with data from additional specimens to balance sample sizes between subspecies and represent the geographic extent of the species more uniformly to assess clinal variation.

Sigmodon f. dalquesti along with *S. f. minimus* Chihuahuan specimen MVZ128460 forms a clade in the maximum likelihood tree with bootstrap support of 98%, which is situated among individuals of *S. f. minimus*. Chihuahuan and New Mexican *S. f. minimus* do not resolve as clades, and branch lengths among *S. f. dalquesti* are very small relative to those among *S. f. fulviventer* from the same series. Overall, the lack of reciprocal monophyly among subspecies is not unexpected; whereas monophyly among mammalian subspecies is not uncommon, a lack of monophyly occurs in instances of relatively recent divergences or frequent admixture. At the same time, although sample sizes were relatively small for each taxon, *S. f. dalquesti* individuals are most closely related to each other and displayed unique haplotypes consistent with many generations of isolation. Also, the two-codon insertion occurring in *S. f. dalquesti* and MVZ128460 (*S. f. minimus*) is probably not selectively neutral and represents a synapomorphy directly linking *S. f. dalquesti* to the main *S. fulviventer* distribution, either as ancestral stock or historical introgression. With a score of 0.4 on the morphological linear discriminate variable (Fig. 3), MVZ128460 was not however morphologically more similar to *S. f. dalquesti* than other *S. f. minimus*.

Pairwise distance calculations between each subspecies are in line with those reported by Bradley and Baker (2001), who reported typical K2P distances for rodent subspecies in the range of 0.00 to 6.29 percent, with a mean of 2.09 percent. The within subspecies values reported in this study are 0.13, 0.36, and 0.73 percent for *S. f. dalquesti*, *S. f. fulviventer*, and *S. f. minimus*, respectively. The values for *S. f. dalquesti* and *S. f. fulviventer* fall within the intrapopulation range reported by Bradley and Baker (2001), whereas the value of 0.73 percent for *S. f. minimus* reflects the intrasubspecific range as expected because populations from New Mexico and Chihuahua are both represented. Notably, the results for *S. f. fulviventer* versus *S. f. minimus* and for *S. f. fulviventer* versus *S. f. dalquesti* both reflect plausible values for intraspecific relationships, the value for *S. f. dalquesti* versus *S. f. minimus* most closely reflect plausible values for intrasubspecific relationships. The lack of available material for *S. f. goldmani* and *S. f. melanotis* as well as the overall modest sample size limits interpretation of these values in the full context of the variation within the species.

The proposed distribution largely matches those previously published in mammalogy literature (Baker 1969; Álvarez-Castañeda et al. 2016). Areas of predicted high relative rate of occurrence (ROR), interpreted as areas on the map with cloglog scores ≥ 0.5, largely agree with published ranges, excepting for substantial areas with high predicted occurrences rates in a region stretching from central New Mexico through northeastern Arizona. Little or no records exist for cotton rats of any species in much of this area, though the fossil record supports members of the genus here in the Blancan stage (Lindsay and Tessman 1974). Other areas not included in published ranges include portions of eastern New Mexico surrounding the Kiowa National Grasslands and a swath of land between US 380 and US 60 north of Roswell, NM, as well as scattered areas between Marfa, TX, and Alamogordo, NM. Further south, the model includes an arc of mostly low-lying agricultural areas north and east of Mexico City. A notable portion of the published ranges that is excluded in the prediction is the northern Chihuahuan Desert west of El Paso/Juarez. Because the cloglog value sharply drops at the boundary of the Chihuahuan Desert precisely where it is defined by the NALCMS land cover data, this is likely an artifact introduced by the categorical nature of the data.

Future trapping effort to confirm the continued presence of the tawny-bellied cotton rat in the Trans-Pecos could benefit from targeted selection of localities based on this distribution model. The initial capture reports from the Fort Davis area come from locations that are at the margins of an area of predicted ROR $\geq$ 0.5. If this population is still present, the model suggests they are more likely to be found in the valley along US-90 between Marfa and Van Horn, TX. Other locations of interest include the Rio Grande River valley between El Paso and Fort Hancock, TX, and the large mesa northeast of Fort Hancock.

Beyond Texas and the immediate scope of this project, the notable areas predicted in New Mexico, Arizona, and Mexico, bear further examination. The San Agustin Basin in New Mexico is predicted to have an ROR ≈ 1. With records of tawny bellied-cotton rats to the north, south, and east, and with plausible corridors that could serve for dispersal, it seems plausible that tawny-bellied cottons rats could occur there (Geluso et al. 2005). The lack of records could be explained by a relative lack of trapping effort in the area. Three potential corridors of dispersal exist: La Jencia Creek, whose drainage begins at the eastern margin of the basin near Magdalena, NM; southwest of Magdalena, the Red Canyon drainage similarly begins at the margins of the basin; at the southern margin of the basin, the Alamosa Creek drainage begins near Oak Peak and Rock Springs Peak. Each of these potential corridors connect to the Rio Grande, and in the case of La Jencia Creek, there is a record of a tawny-bellied cotton rat less than 10 kilometers from where the creek and the river meet. Further potential sites exist in the valleys south-by-southwest of El Malpais National Monument, with potential corridors to known cotton rat occurrence records through the Rio Salado and through El Malpais itself to Grants.

The current analysis incorporates abiotic factors, vegetation, and land cover data. However, a review of the literature suggests that competitive interactions between cotton rat species are likely to play a role in their distributions (Baker 1969; Petersen 197, 1979; Petersen and Helland 1978). The apparent absence of tawny-bellied cotton rats from predicted areas throughout the study area may be explained in part by competitive exclusion. Including range information for these species proved impractical, however. Because of taxonomic

revisions, the ranges of *Sigmodon* sp. in Coahuila, Nuevo Leon, Tamaulipas, Zacatecas, Durango, and Chihuahua are unclear, and the taxonomic identity of observations and specimens recorded for *S. hispidus* in this region is in doubt (Peppers and Bradley 2000; Peppers et al. 2002; Carroll and Bradley 2005; Bradley et al. 2008; Henson and Bradley 2009). When these revisions were made, this problem was clear, however it was not addressed because of a lack of access to genetic material from *Sigmodon* sp. from the area (Bradley et al. 2008). With advances in genetic methods and the increased availability of voucher collection catalogs in online digital databases such as GBIF, this problem may be addressed, though it is beyond the scope of this study.

The totality of evidence gathered from craniometric data and mitochondrial sequences favor recognition of *S. f. dalquesti* as a valid subspecies. Morphometric comparison reveals that statistically significant differences exist between *S. f. dalquesti*, *S. f. minimus*, and *S. f. fulviventer*. Comparison with *S. f. melanotis* failed to reject the null hypothesis in the pairwise PERMANOVA, however examination of the principal coordinates analysis (Fig. 2B) nevertheless suggests a distinction between these two groups. The genetic information suggests that *S. f. dalquesti* is sufficiently distinct from *S. f. minimus*. With three haplotypes among six individuals, the population in Jeff Davis Coounty is unlikely to represent a recent introduction. Principal coordinates ordination of genetic distances suggests a population level affinity with *S. f. minimus* which may indicate that *S. f. dalquesti* originated as an expansion of *S. f. minimus*, or represents a diverging relictual population from a previously more widespread *S. f. minimus*. Node support and a two-codon insertion between a *S. f. minimus* from northern Mexico and *S. f. dalquesti* suggest a geographic route of historical connection. Species distribution modeling predicted a substantially larger range than is currently documented for the tawny-bellied cotton rat. The areas of predicted occurrence should be surveyed to test this distributional hypothesis. Competition between cotton rat species or with other grass-associated rodents such as *Microtus* sp. is a potential explanation of the discrepancy between the recorded and predicated range. If recorded occurrences of Cricetidae can be considered a proxy for sampling effort, then the map (Supplementary Figure 5) of these records suggests that significant areas of *S. fulviventer*'s range are simply under-surveyed. Range extensions of *Sigmodon* continue to be published, so it is plausible that undetected populations exist in the predicted areas.

Field efforts near the type locality were unsuccessful in locating the species. However, as cotton rats are known to be subject to population cycles based on precipitation levels, this may be explainable in terms of persistent drought conditions in the region (Stangl 1992b). A comparison of National Weather Service data on monthly precipitation for the years 1990–1992 and 2017–2019 (Supplementary Data 13) suggest that Stangl's detection occurred in a period of unusually wet conditions, while this study was conducted under dry conditions. Combined with the results of the species distribution model, and with the occurrence of hispid cotton rats in the area, it is plausible that the original detection was a lucky capture at the margin of the range during a population boom cycle. Future field efforts should focus on the areas predicted by the distribution model.

ACKNOWLEDGMENTS

Thanks to Oscar Sandate, Matthew Fox, Craig Tipton, Rachael Wiedmeier, Megan Rowe, Emily Wright, John Stuhler, and Jenna Grimshaw for advice and help in the field. Funding and assistance for this project was generously provided by Texas Parks and Wildlife Department and the United States Fish and Wildlife Service. This project would not have been possible without access to the voucher specimen and tissue collections of the Natural Science Research Laboratory, Midwestern State University, Museum of Southwestern Biology, Museum of Vertebrate Zoology, and National Museum of Natural History. Field work for this project was completed only with the cooperation and support of the Dixon Water Foundation, the Chihuahuan Desert Research Institute, and various private landowners. Museum collection access was coordinated by Ray E. Willis, Chris J. Conroy, Darrin Lunde, Jonathan Dunnum, Mariel Campbell, Heath

Garner, and Kathy MacDonald. Sincere thanks to two anonymous reviewers of an earlier version of this manuscript, whose suggestions were incorporated into the final publication.

Literature Cited

Álvarez-Castañeda, S. T., I. Castro-Arellano, and T. Lacher. 2016. *Sigmodon fulviventer*. The IUCN Red List of Threatened Species 2016.

Amadon, D. 1949. The seventy-five per cent rule for subspecies. The Condor 51:250–258.

Amatulli, G., S. Domisch, M. N. Tuanmu, B. Parmentier, A. Ranipeta, J. Malczyk, and W. Jetz. 2018. A suite of global, cross-scale topographic variables for environmental and biodiversity modeling. Scientific Data 5, article 180040. https://doi.org/10.1038/sdata.2018.40

Anderson, M. J. 2001. A new method for non-parametric multivariate analysis of variance. Austral Ecology 26:32–46.

Anderson, M. J. 2006. Distance-based tests for homogeneity of multivariate dispersions. Biometrics 62:245–253.

Anderson, M. J. 2017. Permutational multivariate analysis of variance (PERMANOVA). Wiley StatsRef: Statistics Reference Online 1–15. https://doi.org/10.1002/9781118445112.stat07841.

Anderson, M. J., K. E. Ellingsen, and B. H. McArdle. 2006. Multivariate dispersion as a measure of beta diversity. Ecology Letters 6:683–693.

Bailey, V. 1913. Ten new mammals from New Mexico. Proceedings of the Biological Society of Washington 26:129–134.

Baker, R. H. 1969. Cotton rats of the *Sigmodon fulviventer* group. Miscellaneous Publications, University of Kansas Museum of Natural History 51:177–232.

Baker, R. H., and K. A. Shump, Jr. 1978. Sigmodon fulviventer. Mammalian Species 94:1–4.

Beal, A. P., and R. S. Pfau. 2016. East meets West: Location of the contact zone between genetic lineages of the cotton rat, *Sigmodon hispidus*, in southeastern Texas. Southwestern Naturalist 61:256–260.

Beauchamp-Martin, S. L., F. B. Stangl, D. S. Schmidly, R. D. Stevens, and R. D. Bradley. 2019. Systematic review of Botta's Pocket Gopher (*Thomomys bottae*) from Texas and southeastern New Mexico, with description of a new taxon. Pp. 515–542 in From field to laboratory: a memorial volume in honor of Robert J. Baker (R. D. Bradley, H. H. Genoways, D. J. Schmidly, and L. C. Bradley, eds.). Special Publications, Museum of Texas Tech University 71.

Benjamini, Y., and Y. Hochberg. 1995. Controlling the false discovery rate - a practical and powerful approach to multiple testing. Journal of the Royal Statistical Society Series B-Methodological 57:289–300.

Bickham, J. W., C. C. Wood, and J. C. Patton. 1995. Biogeographic implications of cytochrome *b* sequences and allozymes in sockeye (*Oncorhynchus nerka*). Journal of Heredity 86:140–144.

Bradley, R. D., and R. J. Baker. 2001. A test of the genetic species concept: cytochrome-*b* sequences and mammals. Journal of Mammalogy 82:960–973.

Bradley, R. D., D. D. Henson, and N. D. Durish. 2008. Re-evaluation of the geographic distribution and phylogeography of the *Sigmodon hispidus* complex based on mitochondrial DNA sequences. Southwestern Naturalist 53:301–310.

Campos, P. F., and T. M. P. Gilbert. 2012. Ancient DNA: methods and protocols. Pp 43–49 in Methods in Molecular Biology (J. Walker ed.). Humana Press, Totowa, New Jersey.

Canada Centre for Remote Sensing, Earth Sciences Sector, Natural Resources Canada,, Comisión Nacional para el Conocimiento y Uso de la Biodiversidad, Comisión Nacional Forestal, Insituto Nacional de Estadística y Geografía, and U.S. Geological Survey. 2013. 2005 Land cover of North America at 250 meters. Commission for Environmental Cooperation, ed..

Carleton, M. D., D. E. Wilson, A. L. Gardner, and M. A. Bogan. 1982. Distribution and systematics of *Peromyscus* (Mammalia:Rodentia) of Nayarit, Mexico. Smithsonian Contributions to Zoology 352:1–46.

Carleton, M. D., R. D. Fisher, and A. L. Gardner. 1999. Identification and distribution of cotton rats, genus *Sigmodon* (Muridae:Sigmodontinae), of Nayarit, Mexico. Proceedings of the Biological Society of Washington 112:813–856.

Carroll, D. S., and R. D. Bradley. 2005. Systematics of the genus *Sigmodon*: DNA sequences from beta-fibrinogen and cytochrome *b*. Southwestern Naturalist 50:342–349.

Center for International Earth Science Information Network. 2018a. Gridded population of the world, version 4 (Gpwv4): Population Count, Revision 11. Palisades: NASA Socioeconomic Data and Applications Center (SEDAC).

Center for International Earth Science Information Network. 2018b. Gridded population of the world, version 4 (Gpwv4): Population Density, Revision 11. NASA Socioeconomic Data and Applications Center (SEDAC), Palisades, New York.

Center for International Earth Science Information Network, and Information Technology Outreach Services. 2013. Global roads open access data set, version 1 (Groadsv1). NASA Socioeconomic Data and Applications Center (SEDAC), Palisades, New York.

Commission for Environmental Cooperation. 2009. Ecological regions of North America. Commission for Environmental Cooperation, ed. Montréal, Canada.

Danecek, P., et al. 2021. Twelve years of SAMtools and BCFtools. Gigascience 10.

Darriba, D., D. Posada, A. M. Kozlov, A. Stamatakis, B. Morel, and T. Flouri. 2019. Modeltest-Ng: a new and scalable tool for the selection of DNA and protein evolutionary models. Molecular Biology and Evolution 37:291–294.

Donath, A., et al. 2019. Improved annotation of protein-coding genes boundaries in metazoan mitochondrial genomes. Nucleic Acids Research 47:10543–10552.

Elwood, R. L., et al. 2007. The American cotton rat: a novel model for pulmonary tuberculosis. Tuberculosis 87:145–154.

Endangered Species Act of 1973. Public Law No. 93-205 (12/28/1973).

Fick, S. E., and R. J. Hijmans. 2017. Worldclim 2: New 1-km spatial resolution climate surfaces for global land areas. International Journal of Climatology 37:4302–4315.

Findley, J. S., and C. J. Jones. 1963. Geographic variation in the least cotton rat in New Mexico. Journal of Mammalogy 44:307–315.

Geluso, K., J. D. Hoffman, V. A. Ashe, J. A. White, and M. A. Bogan. 2005. Westward expansion of the tawny-bellied cotton rat (*Sigmodon fulviventer*) in west-central New Mexico. Southwestern Naturalist 50:273–277.

Henson, D. D., and R. D. Bradley. 2009. Molecular systematics of the genus *Sigmodon*: results from mitochondrial and nuclear gene sequences. Canadian Journal of Zoology 87:211–220.

Hijmans, R. J. 2018. Database of global administrative areas. 3.6 ed.

Jimenez, J. J. 1972. Comparative post-natal growth in five species of the genus *Sigmodon*. II. Cranial character relationships. Revista de Biologia Tropical 20:5–27.

Jin, J. J., W. B. Yu, J. B. Yang, Y. Song, C. W. dePamphilis, T. S. Yi, and D. Z. Li. 2020. GetOrganelle: a fast and versatile toolkit for accurate de novo assembly of organelle genomes. Genome Biology 21:241.

Katoh, K., and D. M. Standley. 2013. MAFFT Multiple sequence alignment software version 7: improvements in performance and usability. Molecular Biology and Evolution 30:772–780.

Koressaar, T., and M. Remm. 2007. Enhancements and modifications of primer design program Primer3. Bioinformatics 23:1289–91.

Kumar, S., G. Stecher, and K. Tamura. 2016. Mega7: Molecular evolutionary genetics analysis version 7.0 for bigger datasets. Molecular Biology and Evolution 33:1870–1874.

Larsson, A. 2014. AliView: a fast and lightweight alignment viewer and editor for large datasets. Bioinformatics 30:3276–3278.

Leary, S. L., et al. 2013. AVMA guidelines for the euthanasia of animals: 2013 Edition. American Veterinary Medical Association, ed.

Li, H., and R. Durbin. 2009. Fast and accurate short read alignment with Burrows-Wheeler transform. Bioinformatics 25:1754–1760.

Lindsay, E. H., and N. T. Tessman. 1974. Cenozoic vertebrate localities and faunas in Arizona. Journal of the Arizona Academy of Science 9:3–24.

Martin, R. E., A. F. DeBlase, and R. H. Pine. 2011. A manual of mammalogy: with keys to families of the world. 3rd ed. Waveland Press, Long Grove, Illinois.

Mayr, E. 1982. Of what use are subspecies. The Auk 99:593–595.

Mayr, E. 1999. Systematics and the origin of species, from the viewpoint of a zoologist [first published 1942]. Harvard University Press, Cambridge.

McDonough, M. M., L. D. Parker, N. R. McInerney, M. G. Campana, and J. E. Maldonado. 2018. Performance of commonly requested destructive museum samples for mammalian genomic studies. Journal of Mammalogy 99:789–802.

Meng, G., Y. Li, C. Yang, and S. Liu. 2019. MitoZ: a toolkit for animal mitochondrial genome assembly, annotation and visualization. Nucleic Acids Research 47:e63–e63.

Merow, C., M. J. Smith, and J. A. Silander. 2013. A practical guide to MaxEnt for modeling species' distributions: what it does, and why inputs and settings matter. Ecography 36:1058–1069.

National Weather Service. 2020. Fort Davis cooperative precipitation 1902–2020.

Odum, E. P. 1955. An eleven year history of a *Sigmodon* population. Journal of Mammalogy 36:368–378.

Okonechnikov, K., O. Golosova, M. Fursov, and UGENE team. 2012. Unipro ugene: a unified bioinformatics toolkit. Bioinformatics 28:1166–1167.

Oksanen, J. F., et al. 2018. Vegan: community ecology package. R package version 2.5-1.

Patten, M. A. 2015. Subspecies and the philosophy of science. The Auk 132:481–485.

Patten, M. A., and P. Unitt. 2002. Diagnosability versus mean differences of sage sparrow subspecies. The Auk 119:26–35.

Peppers, L. L., and R. D. Bradley. 2000. Cryptic species in *Sigmodon hispidus*: evidence from DNA sequences. Journal of Mammalogy 81:332–343.

Peppers, L. L., D. S. Carroll, and R. D. Bradley. 2002. Molecular systematics of the genus *Sigmodon* (Rodentia:Muridae): evidence from the mitochondrial cytochrome-*b* gene. Journal of Mammalogy 83:396–407.

Petersen, M. K. 1973. Interactions between the cotton rats, *Sigmodon fulviventer* and *S. hispidus*. American Midland Naturalist 90:319–333.

Petersen, M. K. 1979. A laboratory test of species exclusion in *Sigmodon fulviventer* and *S. hispidus*. Iowa State Journal of Research 53:301–304.

Petersen, M. K., and M. J. Helland. 1978. Behavioral interactions in *Sigmodon fulviventer* and *S. hispidus*. Journal of Mammalogy 59:118–124.

Phillips, C. D., J. W. Bickham, J. C. Patton, and T. S. Gelatt. 2009. Systematics of Steller Sea Lions (*Eumetopias jubatus*): subspecies recognition based on concordance of genetics and morphometrics. Occasional Papers of the Museum, Texas Tech University 283:1–15.

Phillips, C. D., C. A. Henard, and R. S. Pfau. 2007. Amplified fragment length polymorphism and mitochondrial DNA analyses reveal patterns of divergence and hybridization in the Hispid Cotton Rat (*Sigmodon hispidus*). Journal of Mammalogy 88:351–359.

Phillips, S. J., R. P. Anderson, M. Dudík, R. E. Schapire, and M. E. Blair. 2017. Opening the black box: an open-source release of Maxent. Ecography 40:887–893.

Phillips, S. J., R. P. Anderson, and R. E. Schapire. 2006. Maximum entropy modeling of species geographic distributions. Ecological Modelling 190:231–259.

Phillips, S. J., M. Dudík, J. Elith, C. H. Graham, A. Lehmann, J. Leathwick, and S. Ferrier. 2009. Sample selection bias and presence-only distribution models: implications for background and pseudo-absence data. Ecological Applications 19:181–197.

Pimentel, R. A. 1959. Mendelian infraspecific divergence levels and their analysis. Systematic Zoology 8:139–159.

Prjibelski, A., A. D. Meleshko, A. Lapidus, and A. Korobeynikov. 2020. Using spades de novo assembler. Current Protocols in Bioinformatics 70:e102.

Quinlan, A. R. , and I. M. Hall. 2010. BEDTools: a flexible suite of utilities for comparing genomic features. Bioinformatics 26:841–842.

Rand, A. L., and M. A. Traylor. 1950. The amount of overlap allowable for subspecies. The Auk 67:169–183.

Schmidly, D. J. 1973. Geographic variation and taxonomy of *Peromyscus boylii* from Mexico and the southern United States. Journal of Mammalogy 54:111–130.

Schmidly, D. J., and R. D. Bradley. 2016. The Mammals of Texas. 7th ed. University of Texas Press, Austin.

Sikes, R. S. 2016. 2016 guidelines of the American Society of Mammalogists for the use of wild mammals in research and education. Journal of Mammalogy 97:663–688.

Stamatakis, A. 2014. RAxML version 8: a tool for phylogenetic analysis and post-analysis of large phylogenies. Bioinformatics 30:1312–1313.

Stangl, Jr., F. B. 1992a. First record of *Sigmodon fulviventer* in Texas: natural history and cytogenetic observations. Southwestern Naturalist 37:213–214.

Stangl, Jr., F. B. 1992b. A new subspecies of the Tawny-Bellied Cotton Rat, *Sigmodon fulviventer*, from Trans-Pecos, Texas. Occasional Papers of the Museum, Texas Tech University 145:1–4.

Sullivan, K. A. M., R. N. Platt, R. D. Bradley, and D. A. Ray. 2017. Whole mitochondrial genomes provide increased resolution and indicate paraphyly in deer mice. BMC Zoology 2.

Texas Parks and Wildlife Department. 2012. Texas Conservation Action Plan 2012–2016: Chihuahuan Deserts and Arizona–New Mexico Mountains Handbook, Austin.

Untergasser, A., I. Cutcutache, T. Koressaar, J. Ye, B. C. Faircloth, M. Remm, and S. G. Rozen. 2012. Primer3 - new capabilities and interfaces. Nucleic Acids Research 40:e115–e115.

van Buuren, S., and K. Groothuis-Oudshoorn. 2011. Mice: multivariate imputation by chained equations in R. Journal of Statistical Software 45:1–67.

Venables, W. N., and B. D. Ripley. 2002. Modern Applied Statistics with S. 4th ed. Springer, New York.

Wick, R. R., M. B. Schultz, J. Zobel, and K. E. Holt. 2015. Bandage: interactive visualization of de novo genome assemblies. Bioinformatics 31:3350–3352.

Addresses of authors:

PRESTON J. MCDONALD

Department of Biological Sciences
Texas Tech University
Lubbock, Texas 79409-3131 USA

Current address:
Department of Integrative Biology
University of South Florida
12037 USF Beard Drive, SCA 110
Tampa, Florida 33620 USA
mcdonaldp@usf.edu

KRYSTA DEMERE

Texas Parks and Wildlife Department
Alpine, Texas 79830 USA
krysta.demere@tpwd.texas.gov

RUSSELL MARTIN

Texas Parks and Wildlife Department
Alpine, Texas 79830 USA

JONAH EVANS

Texas Park and Wildlife Department
Austin, Texas 78744 USA
jonah.evans@tpwd.texas.gov

ROBERT D. BRADLEY

Department of Biological Sciences and
Natural Science Research Laboratory
Museum of Texas Tech University
Lubbock, Texas 79409-3131 USA
robert.bradley@ttu.edu

RICHARD D. STEVENS

Department of Natural Resources Management and
Natural Science Research Laboratory
Museum of Texas Tech University
Lubbock, Texas 79409-3131 USA
richard.stevens@ttu.edu

MOHAMED FOKAR

Center for Biotechnology and Genomics
Texas Tech University
Lubbock, Texas 79409-3131 USA
m.fokar@ttu.edu

HENDRA SIHALOHO

Department of Biological Sciences
Texas Tech University
Lubbock, Texas 79409-3131 USA
Hendra.sihaloho@ttu.edu

Caleb D. Phillips

Department of Biological Sciences and
Natural Science Research Laboratory
Museum of Texas Tech University
Lubbock, Texas 79409-3131 USA
caleb.phillips@ttu.edu

Editor for this manuscript was David J. Schmidly

Publications of the Museum of Texas Tech University

This publication is available free of charge in PDF format from the website of the Natural Science Research Laboratory, Museum of Texas Tech University (www.depts.ttu.edu/nsrl). The authors and the Museum of Texas Tech University hereby grant permission to interested parties to download or print this publication for personal or educational (not for profit) use. Re-publication of any part of this paper in other works is not permitted without prior written permission of the Museum of Texas Tech University.

Institutional subscriptions to Occasional Papers are available through the Museum of Texas Tech University, attn: NSRL Publications Secretary, Box 43191, Lubbock, TX 79409-3191. Individuals may also purchase separate numbers of the Occasional Papers directly from the Museum of Texas Tech University.

Series Editor: Robert D. Bradley
Production Editor: Lisa Bradley
Copyright: Museum of Texas Tech University

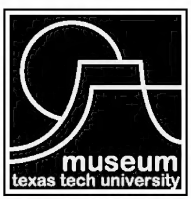

ISSN 0149-175X

Museum of Texas Tech University, Lubbock, TX 79409-3191